



Swansea University  
Prifysgol Abertawe



## Cronfa - Swansea University Open Access Repository

---

This is an author produced version of a paper published in:

*Biochemistry*

Cronfa URL for this paper:

<http://cronfa.swan.ac.uk/Record/cronfa33886>

---

### Paper:

Hughes, R., Johnson, L., Behiry, E., Loveridge, E. & Allemann, R. (2017). A Rapid Analysis of Variations in Conformational Behavior during Dihydrofolate Reductase Catalysis. *Biochemistry*, 56(15), 2126-2133.

<http://dx.doi.org/10.1021/acs.biochem.7b00045>

---

This item is brought to you by Swansea University. Any person downloading material is agreeing to abide by the terms of the repository licence. Copies of full text items may be used or reproduced in any format or medium, without prior permission for personal research or study, educational or non-commercial purposes only. The copyright for any work remains with the original author unless otherwise specified. The full-text must not be sold in any format or medium without the formal permission of the copyright holder.

Permission for multiple reproductions should be obtained from the original author.

Authors are personally responsible for adhering to copyright and publisher restrictions when uploading content to the repository.

<http://www.swansea.ac.uk/iss/researchsupport/cronfa-support/>

# A Rapid Analysis of Variations in Conformational Behavior During Dihydrofolate Reductase Catalysis

Robert L. Hughes, Luke A. Johnson, Enas M. Behiry, E. Joel Loveridge<sup>†</sup> and Rudolf K. Allemann\*

\*School of Chemistry, Cardiff University, Main Building, Park Place, Cardiff CF10 3AT, United Kingdom

<sup>†</sup> Present address: Department of Chemistry, Swansea University, Singleton Park, Swansea SA2 8PP, UK

**KEYWORDS** *Enzyme, catalysis, conformation, dynamics, NMR spectroscopy, isotope labeling*

---

**ABSTRACT:** Protein flexibility is central to enzyme catalysis, yet it remains challenging both to predict conformational behavior based on analysis of amino acid sequence and protein structure and to provide the necessary breadth of experimental support to any such predictions. Here a generic and rapid procedure to identify conformational changes during dihydrofolate reductase (DHFR) catalysis is described. Using DHFR from *Escherichia coli* (EcDHFR), selective side-chain <sup>13</sup>C-labeling of methionine and tryptophan residues is shown to be sufficient to detect the closed-to-occluded conformational transition that follows the chemical step in the catalytic cycle with clear chemical shift perturbations found for both methionine methyl and tryptophan indole groups. In contrast, no such perturbations are seen for the DHFR from the psychrophile *Moritella profunda*, where the equivalent conformational change is absent. Like EcDHFR, *Salmonella enterica* DHFR shows experimental evidence for a large-scale conformational change following hydride transfer that relies on conservation of a key hydrogen bonding interaction between the M20 and GH loops, directly comparable to the closed-to-occluded conformational change observed in EcDHFR. For the hyperthermophile *Thermotoga maritima*, no chemical shift perturbations were observed, suggesting that no major conformational change occurs during the catalytic cycle. In spite of their conserved tertiary structures, DHFRs display variations in the conformational sampling that occurs concurrently with catalysis.

---

Protein motions play important roles in enzyme catalysis and they are often necessary for progression through the catalytic cycle. Originally postulated over half a century ago in Koshland's 'induced fit' model,<sup>1</sup> conformational changes have only more recently been shown to be widely important for substrate binding and product release and to provide an optimal environment for catalysis.<sup>2</sup> Indeed,

multiple enzyme families have been discovered that display conserved motions during catalysis, which indicates evolutionary pressures on both enzyme tertiary structures and the associated dynamics.<sup>3,4</sup> Members of the dihydrofolate reductase (DHFR) class of enzymes are considered to follow similar catalytic cycles and represent a classical enzyme model where conformational changes occur within the catalytic cycle,<sup>5</sup> yet in different DHFR orthologs variations in conformational dynamics have been identified.<sup>6-11</sup> Understanding this diversity of protein motions will in principle help to reveal their importance for the progression through the catalytic cycle and the influence of motions on catalytic proficiency.

DHFRs catalyze transfer of the *pro*-R hydride of reduced nicotinamide adenine dinucleotide phosphate (NADPH) to 7,8-dihydrofolate (DHF) to form 5,6,7,8-tetrahydrofolate (THF). THF acts as a one-carbon shuttle in the metabolism of purines, thymidylate and certain amino acids, and as a result is critical for cellular proliferation. As DHFR is paramount in maintaining the intracellular pool of THF, it has been a long-standing target for both antibacterial and antineoplastic drugs.<sup>12</sup> The canonical DHFR catalytic cycle, derived from studies of *Escherichia coli* DHFR (EcDHFR), exhibits five intermediate complexes<sup>13</sup> that adopt two distinct conformations, namely closed and occluded (Figures 1 & 2).<sup>7</sup> EcDHFR contains three mobile loops within its structure: the highly mobile M20 loop (residues 9-24 by EcDHFR numbering), the FG loop (116-132) and the GH loop (142-149).<sup>7</sup> The holoenzyme (E:NADPH) first binds DHF to form the Michaelis complex (E:NADPH:DHF). In both these intermediates a network of hydrogen bonds between residues in the M20 and FG loops stabilizes a closed conformation,<sup>7</sup> in which the enzyme possesses the optimal electrostatic environment for hydride transfer.<sup>7,14</sup> After product formation these interactions are disrupted and new hydrogen bonds are established between the M20 and GH loops, stabilizing an occluded conformation, which is conserved in the three remaining intermediates (E:NADP<sup>+</sup>:THF, E:THF and

E:THF:NADPH) of the catalytic cycle. Release of NADP<sup>+</sup> and rebinding of NADPH precede the release of THF from the active site, which at pH 7 is the rate limiting step of the reaction.<sup>7</sup> Interchange between the closed and occluded conformations has been shown to modulate affinity for the nicotinamide cofactor and to be important for product release.<sup>7,13,15</sup>

Variations in the conformational changes seen in EcDHFR have been identified in other DHFR homologs. For the DHFR from the psychrophile *Moritella profunda* (MpDHFR), which shares 55% sequence identity with EcDHFR,<sup>16</sup> the catalytic cycle progresses without the enzyme adopting the occluded conformation following hydride transfer,<sup>10</sup> even though the tertiary structures of EcDHFR and MpDHFR are nearly superimposable (Figure 2).<sup>7,17</sup> Crucially, hydrogen bonding between Ser148 and Asn23 is important for stabilizing the occluded conformation; it is abolished in MpDHFR because of a proline residue in place of Ser148.<sup>10</sup> Nonetheless, kinetically MpDHFR follows a similar catalytic cycle to EcDHFR, where release of product is the rate-limiting step under steady state conditions at pH 7.<sup>17</sup> The homodimeric DHFR from the hyperthermophile *Thermotoga maritima* (TmDHFR) exhibits much lower catalytic activity than EcDHFR.<sup>6,18,19</sup> Residues corresponding to the FG loop in TmDHFR form part of the dimer interface and TmDHFR is thought to proceed through the catalytic cycle in an open conformation, although fully conclusive experimental evidence is still lacking.<sup>6,18,19</sup>

Phylogenetic analysis indicates that within bacterial DHFRs there is diversity in whether the hydrogen bond donor and acceptor necessary to permit formation of the occluded conformation are present.<sup>20</sup> Meanwhile, for mammalian DHFRs a proline rich region (PWPP) is inserted into the M20 loop, resulting in diminished flexibility.<sup>11,21,22</sup> This has been demonstrated to affect the stability of the occluded conformation and the N23PP and N23PP/S148A variants of EcDHFR remain in the closed conformation after the chemical step and show reduced catalytic activity (diminished  $k_{cat}$ ) with dissociation of NADP<sup>+</sup> becoming rate limiting.<sup>21</sup> In contrast, EcDHFR-S148P is unable to form an occluded conformation and displays increased product inhibition, but the rate of hydride transfer is not significantly different to that of wild-type EcDHFR.<sup>10</sup> Together these results indicate that while the occluded conformation has little influence on hydride transfer, it is important for modulating cofactor binding affinities and minimizing product inhibition.<sup>10,21</sup> Bacterial DHFRs that conserve the Asn23-Ser148 interaction or possess an equivalent stabilizing interaction should adopt conformations similar to that of the occluded conformation in EcDHFR.<sup>10</sup>

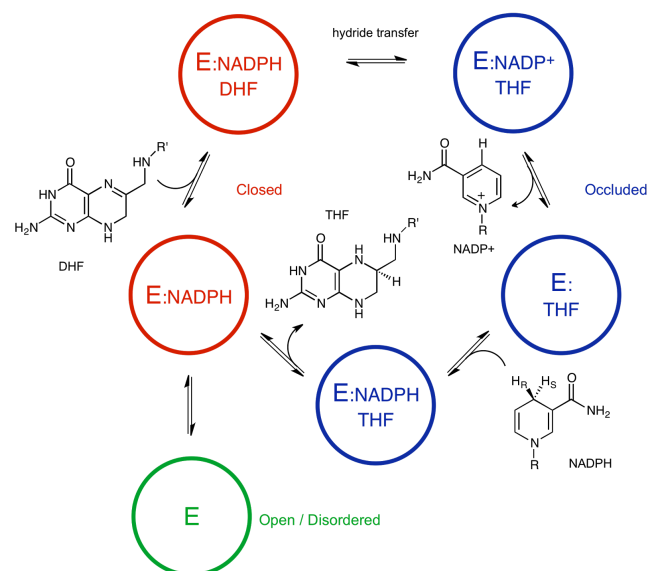


**Figure 1.** The catalytic cycle of EcDHFR under steady state conditions at pH 7. The major protein conformations adopted by the complexes in the catalytic cycle are indicated: open/disordered (green), closed (red) and occluded (blue).<sup>7,23,24</sup>

Although a wealth of kinetic and structural data is available for a number of DHFRs,<sup>5</sup> there currently exists no rapid and cost-effective method to assess enzyme conformational states and loop dynamics for diverse DHFR orthologs. Notably, there are crystal structures of DHFRs from more than 20 organisms,<sup>20</sup> but these structures rarely describe the entire catalytic cycle and are often determined for apo enzymes or solely with the inhibitors methotrexate or trimethoprim. Moreover, for those DHFR structures that are anticipated to lack the occluded conformation, such as those for the enzymes from *Bacillus anthracis*<sup>8</sup> and *Lactobacillus casei*,<sup>25,9</sup> one can only infer differences to the model conformational cycle, since the absence of structural evidence for an occluded conformation does not necessarily imply that the conformation is not adopted. Here we demonstrate that by selective <sup>13</sup>C-labeling of methionine and tryptophan side chains only, conformations in solution can be probed rapidly and highly cost-effectively by NMR spectroscopy at different stages of the catalytic cycle for different DHFR orthologs. The reduced spectral complexity compared to more conventional backbone NMR methods aids interpretation and avoids more cumbersome assignment steps. We show that loop motions essential for progression through the catalytic cycle in EcDHFR are not necessary for efficient catalysis in other orthologs<sup>7,8,25,9,13</sup> and present the first clear experimental evidence in solution that TmDHFR remains in an open conformation throughout the catalytic cycle. Furthermore, we show that DHFR from *Salmonella enterica* (SeDHFR) exhibits similar conformational behavior to EcDHFR, in that it adopts an additional conformation after the chemical step. This work confirms the importance of hydrogen bonding interactions

between the M20 and GH loops in stabilizing alternative occluded-like conformations within the product complex, and demonstrates that EcDHFR is not unique in its ability to switch between conformations.

## MATERIALS AND METHODS

Indole ( $2\text{-}^{13}\text{C}$ ) was purchased from Cambridge Isotope Laboratories. NADP<sup>+</sup> and NADPH were purchased from Melford. DHF was produced by sodium dithionite reduction of folate as described previously.<sup>26</sup> All other chemicals including L-methionine-(*methyl*- $^{13}\text{C}$ ) were from Sigma Aldrich. DHFRs were grown in minimal medium and prepared as previously reported,<sup>17</sup> with the exception of the addition of either L-methionine-(*methyl*- $^{13}\text{C}$ )<sup>27</sup> (80 mg L<sup>-1</sup>) or indole-( $2\text{-}^{13}\text{C}$ )<sup>28</sup> (50 mg L<sup>-1</sup>) at OD<sub>600</sub> 0.4. EcDHFR, MpDHFR and SeDHFR were purified *via* anion exchange chromatography (Q-Sepharose) followed by size exclusion chromatography.<sup>29</sup> For SeDHFR the procedure was adjusted from that published for EcDHFR and is outlined within the Supplementary Information (Figure S1). TmDHFR was purified as previously described.<sup>19</sup> The SeDHFR encoding gene (UNIPROT ID P12833) was purchased from Genscript within the pET-11b vector. The SeDHFR-S150A variant was prepared by standard site-directed mutagenesis methods with the primers (Fwd-5'

GCGGACGATAAGAACGCGTATGCGTGCGAGTTTG  
3' & Rev-5'  
CAAACGCGCACGCATACGCGTTCTTATCGTCCGC  
3'), which were purchased from Sigma-Aldrich and expressed and purified as for wild-type SeDHFR.

All NMR experiments were performed on a Bruker AVANCE III 600 MHz ( $^1\text{H}$ ) spectrometer equipped with a QCI-P cryoprobe and final enzyme concentrations of approximately 250  $\mu\text{M}$ . EcDHFR, MpDHFR and SeDHFR were prepared in 50 mM potassium phosphate buffer (pH 7.0) containing 1 mM NaCl and 10 mM  $\beta$ -mercaptoethanol. TmDHFR was prepared in 50 mM Tris buffer (pH 7.0) containing 1 mM NaCl and 10 mM  $\beta$ -mercaptoethanol. Ligand stocks were pre-prepared at concentrations of 100 mM and pH 7, using extinction coefficients of 6200 cm<sup>-1</sup> M<sup>-1</sup> at 339 nm,<sup>30</sup> 17800 cm<sup>-1</sup> M<sup>-1</sup> at 260 nm,<sup>31</sup> and 28000 cm<sup>-1</sup> M<sup>-1</sup> at 282 nm<sup>32</sup> for NADPH, NADP<sup>+</sup> and folate/DHF, respectively. A ten-fold excess of ligands was used in each NMR experiment and the sample adjusted to pH 7.0 before measurement of the spectra, ensuring saturation (Table S1). To form the E:NADP<sup>+</sup>:THF complex, NADPH and DHF were incubated with the enzyme for 20 minutes at 37 °C, with reaction completion and absence of oxidation products confirmed by  $^1\text{H}$ -NMR. 10% D<sub>2</sub>O was added to all NMR samples. Spectra for MpDHFR, EcDHFR, SeDHFR and TmDHFR were recorded at 7 °C, 25 °C, 25 °C and 40 °C, respectively, in order to maintain sample integrity and to be close to physiological conditions for each enzyme. Spectra were processed with NMRPipe<sup>33</sup> and analyzed using CcpNmr Analysis 2.4.1.<sup>34</sup>

With the exception of Met94, all methionine methyl resonances of MpDHFR had been published previously.<sup>35</sup> The assignment of the Met94 resonances was confirmed and tryptophan indole- $\delta_1$  resonances were assigned by re-evaluation of the 3D  $^{13}\text{C}$ - and  $^{15}\text{N}$ -edited NOESY spectra acquired previously.<sup>35</sup> Each tryptophan indole NH resonance showed an intense NOESY crosspeak to a unique indole- $\delta_1$   $^1\text{H}$  resonance observed here, readily allowing assignment. For EcDHFR, methionine methyl resonances and tryptophan indole- $\delta_1$  resonances for EcDHFR were similarly assigned using 3D  $^{13}\text{C}$ -edited NOESY, CCH-TOCSY and HCCH-TOCSY spectra acquired on a Varian INOVA 800 MHz ( $^1\text{H}$ ) spectrometer equipped with a cryogenically cooled HCN probe, using the 3D  $^{15}\text{N}$ -edited NOESY spectrum acquired previously,<sup>36</sup> and by reference to published data.<sup>37</sup> The equation

$\Delta\delta = \sqrt{\frac{1}{2}[\delta_H^2 + \frac{\delta_C^2}{4}]}$  was used to obtain weighted average chemical shift perturbations.<sup>38</sup>

## RESULTS AND DISCUSSION

To investigate the distribution of protein conformations during the catalytic cycle of different DHFR orthologs, EcDHFR and MpDHFR were first probed as models to identify whether systematic labeling of the proteins with [*methyl*- $^{13}\text{C}$ ] methionine<sup>27</sup> and [indole- $\delta_1$ - $^{13}\text{C}$ ] tryptophan<sup>28</sup> could identify catalytic cycles that include or omit the occluded conformation. The TmDHFR and SeDHFR were investigated to elucidate their conformational behavior, which had not been explored previously. Methionine comprises 3.1% of amino acid residues in MpDHFR and EcDHFR, 2.4% in TmDHFR and 1.8% in SeDHFR, while tryptophan makes up 3.1% of the tryptophan amino acid residues in EcDHFR, 1.9% in MpDHFR and SeDHFR and 0.6% in TmDHFR. This density ensured that a good description of protein conformational space was achieved without significant spectral crowding (Figures 2 and S2).<sup>6,7,17,18</sup> In addition, a number of methionine and tryptophan residues are conserved in structurally significant positions.<sup>6,7,16</sup> Most notably, Trp22 in the M20 loop (Figure S2) is found in a wide range of DHFR orthologs and has been shown to be important for EcDHFR catalysis.<sup>39</sup> Similarly, Met42 is strongly conserved. In total, four of the five methionine residues in EcDHFR are conserved in MpDHFR (Met1, Met20, Met42 and Met92) and three of the five are conserved in SeDHFR (Met1, Met42 and Met92), although only Met44 is conserved in TmDHFR (Figure S2). The remaining two methionines in TmDHFR are located within the dimer interface. In addition to Trp22, EcDHFR, MpDHFR and SeDHFR possess a Trp133 equivalent, although other tryptophan residues are well dispersed throughout the protein structure. Met1 in TmDHFR is mostly removed during expression by an aminopeptidase present in *E. coli* (Figure S3).<sup>40</sup>

$^1\text{H}$ - $^{13}\text{C}$  HSQC spectra of EcDHFR labeled with [*methyl*- $^{13}\text{C}$ ] methionine or [indole- $\delta_1$ - $^{13}\text{C}$ ] tryptophan

(Figure 3A and 3B, Tables S2 and S3) exhibit five distinct cross-peaks corresponding to the five methionine and five tryptophan residues when in the presence of ligands. The spectrum for [*methyl*-<sup>13</sup>C] methionine labeled apo-enzyme was of lower quality, with multiple minor cross-peaks observed for some residues (Figure S5). This is characteristic of spectra of apo-EcDHFR and apo-MpDHFR where the enzyme is in slow exchange between multiple conformational states.<sup>36,41</sup> Addition of ligands (NADP<sup>+</sup> and folate to model the Michaelis complex, or NADP<sup>+</sup> and THF to form the product ternary complex) resulted in increased spectral quality, reduction of the number of cross-peaks and increased resolution.<sup>36</sup> Complex formation also led to significant changes in chemical shift, indicative of the enzyme transitioning to a new conformation. Dramatic changes in chemical shift were also observed between the E:NADP<sup>+</sup>:folate and E:NADP<sup>+</sup>:THF complexes, as the enzyme progressed to an occluded conformation after the chemical step. The largest chemical shift perturbations were exhibited by Met20 and Trp22, located in the highly flexible M20 loop; Met16, Met92 and Trp133 also showed notable changes.

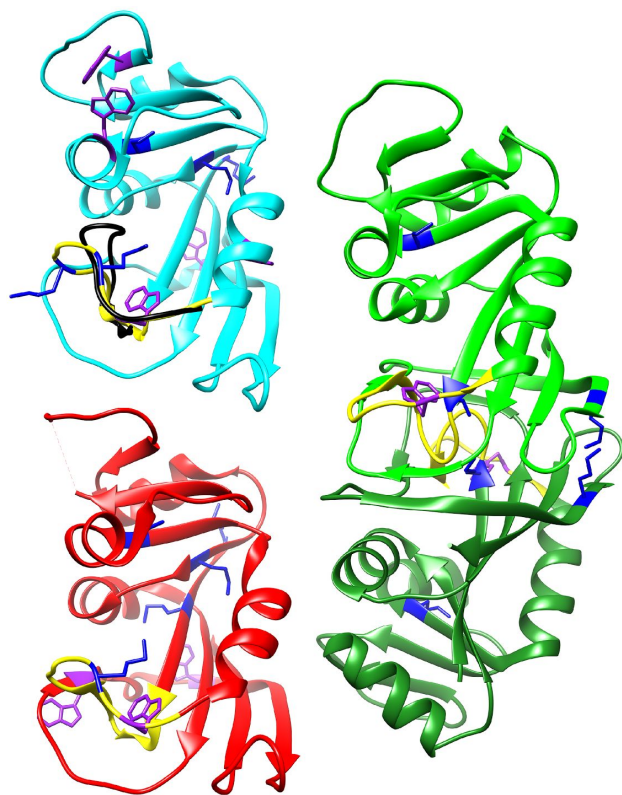


**Figure 2.** Cartoon representations of EcDHFR (cyan, PDB 1RX2<sup>7</sup>), TmDHFR (green, PDB 1D1G<sup>6</sup>) and MpDHFR (red, PDB 3IA5<sup>29</sup>). The ‘M20’ loop in the occluded (black) and closed (yellow) conformations is highlighted as well as positions of methionine (blue) and tryptophan (purple).

As with the spectrum of [*methyl*-<sup>13</sup>C] methionine labeled apo-EcDHFR, the <sup>1</sup>H-<sup>13</sup>C HSQC spectra of apo-MpDHFR labeled with [*methyl*-<sup>13</sup>C] methionine or [*indole*- $\delta_1$ -<sup>13</sup>C]

tryptophan exhibited clear evidence of conformational heterogeneity (Figure S5). Again, addition of ligands led to an increase in spectral quality, indicative of the enzyme adopting one major conformation. <sup>1</sup>H-<sup>13</sup>C-HSQC spectra of the two complexes showed the expected five methionine and three tryptophan cross-peaks (Figures 3C and 3D). No significant change in chemical shift was observed between the Michaelis and product complexes for methionine or tryptophan residues (Tables S4 and S5). Notably, small changes in proton chemical shifts for Met21 and Trp23 were observed but as these residues are directly adjacent to the site of chemistry these most likely occur because of the differences in ligands, highlighting how it is important to differentiate between small changes that describe the changes at the site of chemistry and more widespread chemical shift deviations, indicative of protein conformational changes as observed for EcDHFR.

The extensive differences in chemical shifts seen in the EcDHFR:NADP<sup>+</sup>:folate and EcDHFR:NADP<sup>+</sup>:THF complexes, as had previously been observed for <sup>15</sup>N-alanine labeled EcDHFR,<sup>42</sup> provide clear evidence that methionine and tryptophan labeling is sufficient to observe the closed-to-occluded conformational change in EcDHFR. As expected, residues in the flexible M20 loop (Met16, Met20 and Trp22) all show large changes. Met16 in the apo-enzyme and Michaelis complex appears to be solvent exposed. However, in the product complex the residue is located directly within the active site,<sup>7</sup> drastically changing the immediate molecular environment of the <sup>13</sup>C-methyl group. Again, Met20 in the Michaelis complex points towards the FG loop, whereas in the product complex it is more solvent exposed, thus accounting for the observed downfield shift. Importantly, in EcDHFR chemical shift changes are widely observed for all methionine and most tryptophan resonances, allowing binding effects of different ligands and deviations in protein conformation to be differentiated. No such widespread and significant changes in chemical shift were observed between the MpDHFR:NADP<sup>+</sup>:folate and MpDHFR:NADP<sup>+</sup>:THF complexes, confirming earlier work that suggested that MpDHFR does not adopt an occluded conformation after hydride transfer.<sup>10</sup> The results gained from EcDHFR and MpDHFR confirm that selective side-chain labeling can be used to identify whether an occluded-like conformation is adopted by a specific DHFR.

It has so far been challenging to investigate TmDHFR by conventional NMR methods due poor tumbling in solution and fast *T*<sub>2</sub> relaxation as a consequence of its dimeric nature with a total molecular mass of 38k and its elongated shape.<sup>18</sup> Perdeuteration of TmDHFR in order to improve relaxation issues proved ineffective as the high thermal stability of TmDHFR prevented complete proton back-exchange of backbone amide groups in non-solvent exposed regions (Figure S4). Consequently, three-dimensional NMR spectra of TmDHFR are of limited quality and no triple resonance assignment data for

TmDHFR have been published. However, TmDHFR only contains three methionines and one tryptophan.<sup>18</sup> Since these side chains display superior relaxation properties, selective side-chain labeling can be used to explore the conformational dynamics of TmDHFR. <sup>1</sup>H-<sup>13</sup>C HSQC spectra of TmDHFR exhibit four distinct methionine cross-peaks and one tryptophan cross peak (Figures 3E and 3F). Met1 could be assigned as this resonance was considerably lower in intensity than the others, as expected for a residue only present in ~10% of the protein molecules due to amino-peptidase activity in *E. coli* (Figure S3). No significant changes in [*methyl*-<sup>13</sup>C] methionine chemical shift were observed between the apo-enzyme and either complex (Tables S6 and S7). Trp23 displays a proton shift difference of 0.07 ppm between the Michaelis and product complexes, similar to that observed for MpDHFR. This difference is most likely due to different ligands, which are directly proximal to Trp23. These results suggest that TmDHFR adopts only a single major conformation in solution.

The occluded conformation has so far only been in EcDHFR, although some evidence of conformational flexibility following the chemical step has been reported for bacterial DHFRs.<sup>11</sup> We therefore tested our proposal that DHFR homologs that can form a hydrogen bond similar to the crucial Ser148-Asn23 interaction in EcDHFR, will adopt a conformation similar to the occluded conformation found in EcDHFR. SeDHFR contains residues His24 and Ser150 in the equivalent positions (Figure S2) and the replacement of asparagine by histidine is not likely to have a negative effect because the hydrogen bonds are formed to the backbone amide and carbonyl of Asn23. SeDHFR should therefore adopt an occluded-like conformation following the chemical step. No NMR assignments or structural information currently exist for SeDHFR, although tentative assignment of methionine residues could be performed *via* sequence analysis indicating that conserved residues are likely to reside in similar electronic environments to those in EcDHFR and MpDHFR. Like EcDHFR and MpDHFR, [*methyl*-<sup>13</sup>C] spectra of methionine labeled SeDHFR apo-enzyme were of low quality as a consequence of conformational heterogeneity (Figure S5). SeDHFR exhibits three well defined cross peaks when in the E:NADP<sup>+</sup>:folate complex. However, unlike EcDHFR, SeDHFR shows two distinct species in the E:NADP<sup>+</sup>:THF complex; both species seem to be equally populated (Figures 3G and 3H). Half of the cross peaks present in the product complex overlap with those present in the Michaelis complex, indicating that in the product complex SeDHFR is characterized by an equilibrium between the Michaelis conformation and a second conformational state (Tables S8 and S9). It is worthy of note that changing Ser148 in EcDHFR leads to a destabilization of the occluded conformation.<sup>21</sup> To confirm whether the two observed species in SeDHFR related to similar conformational behavior, SeDHFR-S150A was

prepared. In the product complex, two species were present in this variant, but the relative population of the two states was drastically shifted to favor the Michaelis complex (Figures 3I and 3J, Tables S10 and S11). This reinforced that the chemical shift perturbations observed in Met94 and Met42 are likely to be caused by a conformational change resembling that found in EcDHFR, and again confirmed the significance of the hydrogen bond interaction between the M20 and GH loops in its formation. No significant chemical shift perturbations were observed in the [indole- $\delta_1$ -<sup>13</sup>C] tryptophan labeled SeDHFR, which in this instance proved not to be diagnostic of conformational change.

SeDHFR, unlike EcDHFR and MpDHFR, lacks methionine residues within the M20 loop, which directly participates in the closed-to-occluded conformational change. To provide further evidence that the second conformation present in the product complex of SeDHFR resembles the occluded conformation observed for EcDHFR, <sup>1</sup>H-<sup>15</sup>N HSQC spectra were acquired of both the Michaelis and product complexes (Figures S6 and S7). As observed through the [*methyl*-<sup>13</sup>C] methionine resonances, widespread chemical shift differences are found between the complexes; again justifying that simple side chain labeling is sufficient to identify conformational change within DHFRs, even when the probes are not located directly within the site of conformation change. This suggested that SeDHFR does indeed form an occluded-like conformation.

In general, we found [*methyl*-<sup>13</sup>C] methionine chemical shifts more diagnostic of DHFR conformational changes than those of [indole- $\delta_1$ -<sup>13</sup>C] tryptophan. In all four DHFRs, Trp22 forms a hydrogen bond to bound folates. It would therefore be expected to show a difference in chemical shift between the apo-enzyme and the two complexes. In MpDHFR and TmDHFR Trp23 does indeed display small proton chemical shifts for each separate complex, while in contrast no significant differences are observed for SeDHFR. A large deviation is found for the Michaelis complex of EcDHFR, but apo-enzyme and product complexes are similar. Taken together this illustrates how ligand binding effects dominate for this residue due to its location adjacent to the site of chemistry, obscuring any chemical shift perturbations in response to protein conformational changes. Similarly, for the spectra of apo-EcDHFR, MpDHFR and SeDHFR, the tryptophan data show no evidence of the conformational heterogeneity obviously present when observing [*methyl*-<sup>13</sup>C] methionine spectra and which has been previously reported.<sup>28,43</sup> Conformational changes can nonetheless be followed through [indole- $\delta_1$ -<sup>13</sup>C] tryptophan labeling, since there is clear evidence for the closed-to-occluded transition in EcDHFR, which may simply be more evident for EcDHFR than SeDHFR due to the larger number of [indole- $\delta_1$ -<sup>13</sup>C] tryptophans present within its sequence.

Importantly, by combining the [indole- $\delta_1$ - $^{13}\text{C}$ ] tryptophan labeling with [*methyl*- $^{13}\text{C}$ ] methionine labeling, which could in principle have been performed in a single protein, clear evidence of large-scale protein conformational changes was found for EcDHFR and ScDHFR. In EcDHFR the capability to switch to an occluded conformation is essential for progression through the catalytic cycle, but this had not previously been observed in other DHFRs.<sup>10,11</sup> Ser148 in EcDHFR, which forms two hydrogen bonds to the M20 loop, is replaced by proline in MpDHFR.<sup>10</sup> Consequently M20 loop motions appear not to play a significant role in MpDHFR catalysis, and it was known that MpDHFR remains in a closed conformation throughout the catalytic cycle.<sup>10,44</sup> Switching from the

closed to the occluded conformation immediately follows hydride transfer in EcDHFR, before release of  $\text{NADP}^+$  from the product ternary complex.<sup>45</sup> Switching to the occluded conformation in EcDHFR lowers the binding affinity of  $\text{NADP}^+$ , mitigates possible product inhibition effects and allows efficient progress through the catalytic cycle.<sup>10,46</sup> However, similar single turnover rate constants for EcDHFR- and MpDHFR-catalyzed hydride transfer at pH 7 show that the ability to form the occluded conformation does not have a major effect on the chemical step. Hydride transfer in the occluded conformation is not possible due to the distance between the reactants.<sup>10,36</sup>

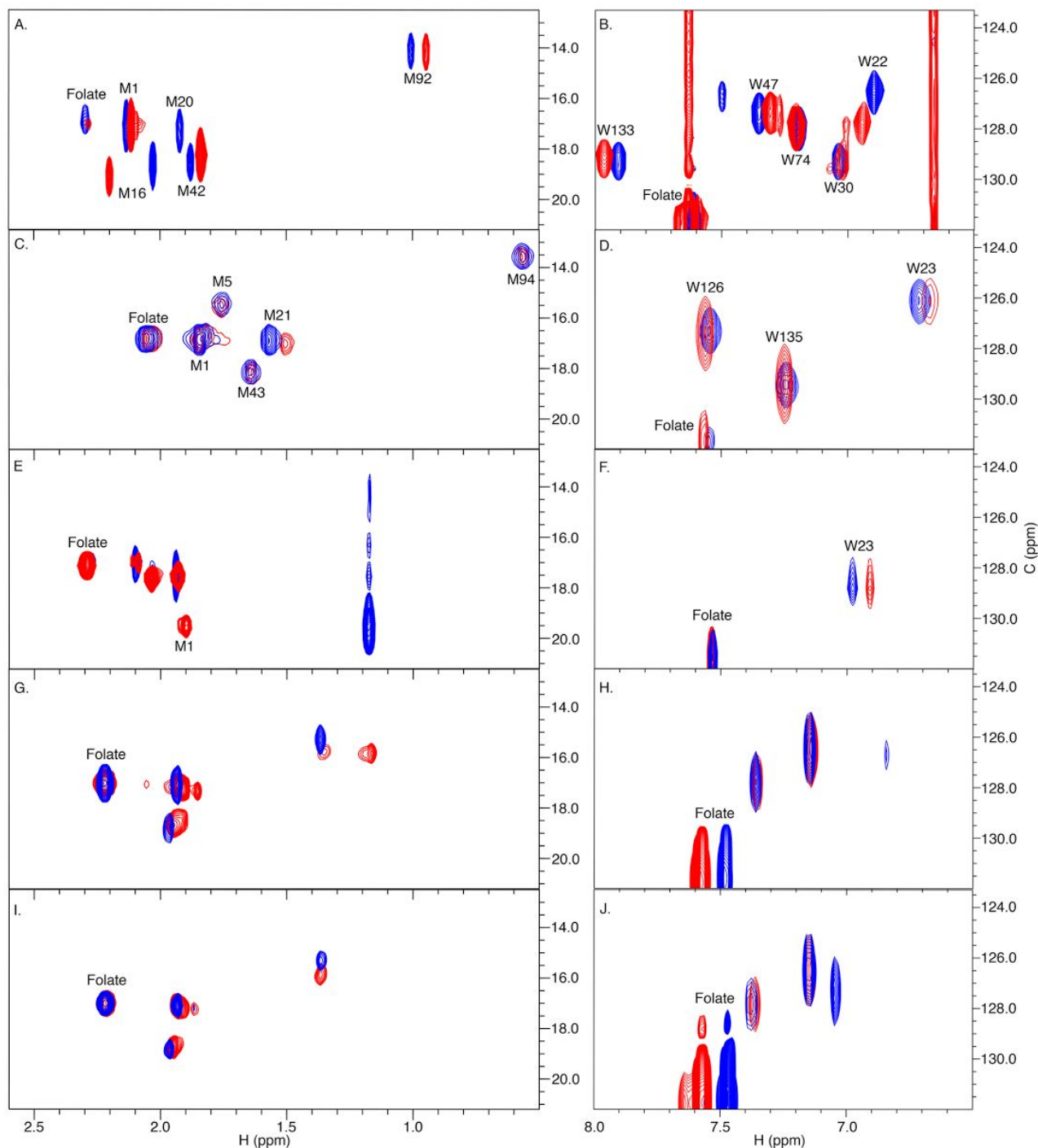


**Figure 3.**  $^1\text{H}$ - $^{13}\text{C}$  HSQC spectra of  $^{13}\text{C}$  labeled DHFR complexes, E:NADP<sup>+</sup>:folate (closed conformation in EcDHFR) (blue) and E:NADP<sup>+</sup>:THF (occluded conformation in EcDHFR) (red). (A) [*methyl*- $^{13}\text{C}$ ] methionine labeled EcDHFR, (B) [ $\delta_1$ - $^{13}\text{C}$ ] tryptophan labeled EcDHFR, (C) [*methyl*- $^{13}\text{C}$ ] methionine labeled MpDHFR, (D) [ $\delta_1$ - $^{13}\text{C}$ ] tryptophan labeled MpDHFR, (E) [*methyl*- $^{13}\text{C}$ ] methionine labeled TmDHFR, (F) [ $\delta_1$ - $^{13}\text{C}$ ] tryptophan labeled TmDHFR, (G) [*methyl*- $^{13}\text{C}$ ] methionine labeled SeDHFR, (H) [ $\delta_1$ - $^{13}\text{C}$ ] tryptophan labeled SeDHFR, (I) [*methyl*- $^{13}\text{C}$ ] methionine labeled SeDHFR-S150A, (J) [ $\delta_1$ - $^{13}\text{C}$ ] tryptophan labeled SeDHFR-S150A.

Despite the lack of assignment data for both Tm- and SeDHFR, important conclusions can be drawn from the data presented here. Side chain labeling of methionine and tryptophan yields simple and intuitively useful data. Previous reports that TmDHFR remains in a fixed open

conformation during catalysis were based upon two X-ray single crystal structures and neither of them effectively modeled the Michaelis or product complex.<sup>18</sup> Hence here the first direct evidence is reported that TmDHFR remains fixed in an open conformation throughout the catalytic



cycle. Any further emphasis is however limited for TmDHFR due to the different distribution of methionine residues to Ec- and MpDHFR, and highlights how the distribution and conservation of labels can be potentially limiting when establishing conformational changes and comparing orthologs.

The ease of labeling meant that the conformational behavior of SeDHFR, for which no structural data exists, could be analyzed rapidly and predictions based upon primary sequence analysis were verified. SeDHFR exists in multiple solution forms and their assignment could be based on similarity to other DHFRs. Like EcDHFR, SeDHFR showed two conformations in the product complex but the relative stability of two conformations was evidently different. The occluded conformation dominates in the product complex of EcDHFR, while in SeDHFR the Michaelis conformation is still present in approximately equimolar concentration. This difference may influence the kinetics of product release.

Principally selective side-chain  $^{13}\text{C}$ -labeling provides a rapid and cost effective approach to survey protein conformations during catalysis for multiple proteins, allowing more traditional and detailed analysis to be adjudged worthwhile. The cost of production of [*methyl*- $^{13}\text{C}$ ] methionine (£11 per liter of culture) and [*indole- $\delta_1$* - $^{13}\text{C}$ ] tryptophan (£96 per liter of culture) labeled proteins is considerably lower than that of triply ( $^2\text{H}$ ,  $^{13}\text{C}$ ,  $^{15}\text{N}$ , £622 per liter of culture) or doubly ( $^{13}\text{C}$ ,  $^{15}\text{N}$ , £262 per liter of culture) labeled proteins required for full NMR assignments, (when accounting for 4 g L $^{-1}$  U- $^2\text{H}$ ,  $^{13}\text{C}$  and U- $^1\text{H}$ ,  $^{13}\text{C}$  glucose respectively). Selective labeling also provides greatly simplified spectra, exhibiting only a fraction of the number of cross-peaks seen for fully labeled proteins and the data can be acquired over much narrower spectral windows (10-14 ppm in  $^{13}\text{C}$  rather than ~70 ppm for a full aliphatic  $^1\text{H}$ - $^{13}\text{C}$  HSQC). In addition,  $^{13}\text{CH}_3$  groups (as in [*methyl*- $^{13}\text{C}$ ] methionine) typically show high sensitivity in NMR experiments, due to the three equivalent protons<sup>43</sup> and aliphatic  $^{13}\text{C}$  shifts are most sensitive to conformational changes.<sup>38</sup> For DHFR, selective side chain  $^{13}\text{C}$ -labeling is clearly sufficient to gain insight into large-scale protein motions that are important for progression through the catalytic cycle, and expands upon previous work which demonstrated for EcDHFR the effectiveness of side chain labeling methods in measuring ps – ns timescale protein dynamics.<sup>47</sup>

In conclusion we have demonstrated here the utility of selective side-chain labeling to rapidly probe conformational behavior during DHFR catalysis. EcDHFR is known to undergo large-scale conformational changes along the catalytic cycle and shows clear chemical shift perturbations of its methionine methyl and tryptophan indole groups following the chemical step. MpDHFR, on the other hand, an enzyme known to maintain a single major conformation during catalysis, does not display such perturbations. Thermostable, homodimeric TmDHFR does

not show any significant chemical shift perturbations following the chemical step, corroborating crystallographic evidence and providing the first direct evidence that this enzyme also adopts a single major conformation in solution. Conformational sampling is however not unique to EcDHFR and DHFR from *Salmonella enterica* exhibits similar conformational behavior, most likely adopting an occluded-like conformation. Clearly, amino acid sequence analysis allows the prediction of large-scale protein conformational behavior in DHFRs and spectra obtained with site selectively labeled proteins may be readily interpreted even in the absence of resonance assignments. However, the scope of selective side-chain  $^{13}\text{C}$ -labeling is not limited to an analysis of structural events during DHFR catalysis, and can be used to track conformational changes in a wide range of proteins.

## ASSOCIATED CONTENT

### Supporting Information.

Purification procedure for SeDHFR and SDS-PAGE gel; amino acid sequence analysis of multiple DHFRs; mass spectrum of TmDHFR highlighting the presence of Met1; a modified version of Figure 3 including spectra for APO complexes;  $^1\text{H}$ - $^{15}\text{N}$  HSQC spectra of SeDHFR in both the Michaelis and product complexes and tables cataloguing the observed weighed chemical shift changes.

## AUTHOR INFORMATION

### Corresponding Authors

R.K.A.: School of Chemistry, Cardiff University, Main Building, Park Place, Cardiff CF10 3AT, UK. E-mail: allemannrk@cardiff.ac.uk. Phone: (44) 29 2087 9014.

### Author Contributions

R.L.H. performed the experimental work. R.L.H., L.A.J., E.M.B, E.J.L. and R.K.A. designed the experiments and composed the manuscript.

### Funding Sources

This work was supported by the U.K. Biotechnology and Biological Sciences Research Council (BBSRC) through grants BB/J005266/1, BB/L020394/1 and BB/M006158/1, by the Life Sciences Research Network Wales (an initiative funded through the Welsh Government's Sêr Cymru programme) and by Cardiff University.

### Notes

The authors declare no competing financial interests.

## ACKNOWLEDGMENT

We thank Dr Sara Whittaker of the Biomolecular NMR Facility at the University of Birmingham for assistance with the operation of the Varian INOVA 800 MHz ( $^1\text{H}$ ) spectrometer. The help of Dr Rob Jenkins and Mr Thomas

Williams with mass spectrometry and NMR spectroscopy is gratefully acknowledged.

## ABBREVIATIONS

DHFR, dihydrofolate reductase; EcDHFR, DHFR from *E. coli*; MpDHFR, DHFR from *M. profunda*; TmDHFR, DHFR from *T. maritima*; SeDHFR, DHFR from *S. enterica*; NADP<sup>+</sup>, nicotinamide adenine dinucleotide phosphate; NADPH, nicotinamide adenine dinucleotide phosphate (reduced form); DHF, dihydrofolate; THF, tetrahydrofolate; PDB, Protein data bank.

## REFERENCES

- (1) Koshland, D. E. (1958) Application of a theory of enzyme specificity to protein synthesis. *Proc. Natl. Acad. Sci.* 44, 98–104.
- (2) Karplus, M., and McCammon. (1983) Dynamics of Proteins: Elements and Function. *Annu. Rev. Biochem.* 53, 263–300.
- (3) Sawaya, M. R., and Kraut, J. (1997) Loop and subdomain movements in the mechanism of *Escherichia coli* dihydrofolate reductase: Crystallographic evidence. *Biochemistry* 36, 586–603.
- (4) Katebi, A. R., and Jernigan, R. L. (2014) The critical role of the loops of triosephosphate isomerase for its oligomerization, dynamics, and functionality. *Protein Sci.* 23, 213–218.
- (5) Luk, L. Y. P., Loveridge, E. J., and Allemann, R. K. (2015) Protein motions and dynamic effects in enzyme catalysis. *Phys. Chem. Chem. Phys.* 17, 30817–30827.
- (6) Dams, T., Auerbach, G., Bader, G., Jacob, U., Ploom, T., Huber, R., and Jaenicke. (2000) The crystal structure of dihydrofolate reductase from *Thermotoga maritima*: molecular features of thermostability. *R. J. Mol. Biol.* 297, 659–672.
- (7) Sawaya, M. R., and Kraut, J. (1997) Loop and subdomain movements in the mechanism of *Escherichia coli* dihydrofolate reductase: Crystallographic evidence. *Biochemistry* 36, 586–603.
- (8) Beierlein, J. M., Frey, K. M., Bolstad, D. B., Pelphrey, P. M., Joska, T. M., Smith, A. E., Priestley, N. D., Wright, D. L., and Anderson, A. C. (2008) Synthetic and Crystallographic Studies of a New Inhibitor Series Targeting *Bacillus anthracis* Dihydrofolate Reductase. *J. Med. Chem.* 51, 7532–7540.
- (9) Feeney, J., Birdsall, B., Kovalevskaya, N. V., Smurnyy, Y. D., Navarro Peran, E. M., and Polshakov, V. I. (2011) NMR Structures of Apo *L. casei* Dihydrofolate Reductase and its Complexes with Trimethoprim and NADPH: Contributions to Positive Cooperative Binding from Ligand-Induced Refolding, Conformational Changes, and Interligand Hydrophobic Interactions. *Biochemistry* 50, 3609–3620.
- (10) Behiry, E. M., Luk, L. Y. P., Matthews, S. M., Loveridge, E. J., and Allemann, R. K. (2014) Role of the occluded conformation in bacterial dihydrofolate reductases. *Biochemistry* 53, 4761–4768.
- (11) Bhabha, G., Ekiert, D., Jennewein, M., Zmasek, C. M., Tuttle, L. M., Kroon, G., Dyson, J. H., Godzik, A., Wilson, I. A., and Wright, P. E. (2013) Divergent evolution of protein conformational dynamics in dihydrofolate reductase. *Nat. Struct. Mol. Biol.* 20, 1243–1249.
- (12) Blakley, R. L. (1984) in *Folates and Pterins* pp 191–253, Wiley, New York.
- (13) Fierke, C. A., Johnson, K. A., and Benkovic, S. J. (1987) Construction and Evaluation of the Kinetic Scheme Associated with Dihydrofolate reductase from *Escherichia coli*. *Biochemistry* 26, 4085–4092.
- (14) Loveridge, E. J., Behiry, E. M., Guo, J., and Allemann, R. K. (2012) Evidence that a 'Dynamic Knockout' in *Escherichia coli*

Dihydrofolate Reductase does not affect the chemical step of catalysis. *Nat. Chem.* 4, 292–297.

- (15) McElheny, D., Schnell, J. R., Lansing, J. C., Dyson, H. J., and Wright, P. E. (2005) Defining the role of active-site loop fluctuations in dihydrofolate reductase catalysis. *Proc. Natl. Acad. Sci. U. S. A.* 102, 5032–5037.
- (16) Xu, Y., Feller, G., Gerday, C., and Glansdorff, N. (2003) *Moritella* Cold-Active Dihydrofolate Reductase: Are There Natural Limits to Optimization of Catalytic Efficiency at low temperatures? *J. Bacteriol.* 185, 5519–5526.
- (17) Evans, R. M., Behiry, E. M., Tey, L. H., Guo, J., Loveridge, E. J., and Allemann, R. K. (2010) Catalysis by dihydrofolate reductase from the psychropiezophile *Moritella profunda*. *ChemBioChem* 11, 2010–2017.
- (18) Dams, T., Bohm, G., Auerbach, G., Bader, G., Schurig, H., and Jaenicke, R. (1998) Homo-dimeric recombinant dihydrofolate reductase from *Thermotoga maritima* shows extreme intrinsic stability. *Biol. Chem.* 379, 367–371.
- (19) Maglia, G., Javed, M. H., and Allemann, R. K. (2003) Hydride Transfer During Catalysis by Dihydrofolate Reductase from *Thermotoga maritima*. *Biochem. J.* 374, 529–535.
- (20) Hecht, D., Tran, J., Fogel, G. B. (2011) Structural-based analysis of dihydrofolate reductase evolution. *Mol. Phylogenet. Evol.* 61, 212–230.
- (21) Bhabha, G., Lee, J., Ekiert, D. C., Gam, J., Wilson, I. A., Dyson, H. J., Benkovic, S. J., and Wright, P. E. (2011) A dynamic knockout reveals that conformational fluctuations influence the chemical step of enzyme catalysis. *Science* 332, 234–238.
- (22) Liu, C. T., Hanoian, P., French, J. B., Pringle, T. H., Hammes-Schiffer, S., and Benkovic, S. J. (2013) Functional significance of evolving protein sequence in dihydrofolate reductase from bacteria to humans. *Proc. Natl. Acad. Sci. U. S. A.* 110, 10159–10164.
- (23) Falzone, C. J., Wright, P. E., and Benkovic, S. J. (1994) Dynamics of a flexible loop in dihydrofolate reductase from *Escherichia coli* and its implication for catalysis. *Biochemistry* 33, 439–442.
- (24) Li, L., Falzone, C. J., Wright, P. E., and Benkovic, S. J. (1992) Functional Role of a Mobile Loop of *Escherichia coli* Dihydrofolate reductase in Transition State Stabilization. *Biochemistry* 31, 7826–7833.
- (25) Gargaro, A. R., Soteriou, A., Frenkiel, T. A., Bauer, C. J., Birdsall, B., Polshakov, V. I., Barsukov, I. L., Roberts, G. C., and Feeney, J. (1998) The Solution Structure of the Complex of *Lactobacillus Casei* Dihydrofolate Reductase with Methotrexate. *J. Mol. Biol.* 277, 119–134.
- (26) Blakley, R. L. (1960) Crystalline dihydropteroylglutamic acid. *Nature* 188, 231–232.
- (27) Tzeng, S. R., Pai, M. T., and Kalodimos, C. G. (2012) NMR Studies of Large Protein Systems. *Methods Mol. Biol.* 831, 133–140.
- (28) Rodriguez-Mias, R. A., and Pellicchia, M. (2003) Use of Selective Trp Side Chain Labeling To Characterize Protein-Protein and Protein-Ligand Interactions by NMR Spectroscopy. *J. Am. Chem. Soc.* 125, 2892–2893.
- (29) Hay, S., Evans, R. M., Levy, C., Loveridge, E. J., Wang, X., Leys, D., Allemann, R. K., and Scrutton, N. S. (2009) Are the catalytic properties of enzymes from piezophilic organisms pressure adapted? *ChemBioChem* 10, 2348–2353.
- (30) Allemann, R. K., Evans, R. M., Tey, L., Maglia, G., Pang, J., Rodriguez, R., Shrimpton, P. J., and Swanwick, R. S. (2006) Protein Motions During Catalysis by Dihydrofolate Reductases. *Philos. Trans. Roy. Soc. B.* 361, 1317–1321.
- (31) Wang, X., Chan, T. F. A. I., and Lam, V. M. S. (2008) What is the role of the second "Structural" NADP<sup>+</sup> binding site in

human glucose 6-phosphate dehydrogenase? *Protein Sci.* 17, 1403–1411.

(32) Zakrzewski, S. F., and Sansone, A. M. (1971) A new synthesis of tetrahydrofolic acid. *Methods Enzymol.* 18, 728–731.

(33) Delaglio, F.; Grzesiek, S.; Vuister, G. W.; Zhu, G.; Pfeifer, J., and Bax, A. (1995) Nmrpipe: A Multidimensional Spectral Processing System Based on Unix Pipes. *J. Biomol. NMR* 6, 277–293.

(34) Vranken, W. F., Boucher, W., Stevens, T. J., Fogh, R. H., Pajon, A., Llinas, M., Ulrich, E. L., Markley, J. L., Ionides, J., and Laue, E. D. (2005) The CCPN data model for NMR spectroscopy: Development of a software pipeline. *Proteins Struct. Funct. Genet.* 59, 687–696.

(35) Loveridge, E. J., Matthews, S. M., Williams, C., Whittaker, S. B. M., Günther, U. L., Evans, R. M., Dawson, W. M., Crump, M. P., and Allemann, R. K. (2013) Aliphatic <sup>1</sup>H, <sup>13</sup>C and <sup>15</sup>N chemical shift assignments of Dihydrofolate reductase from the psychropiezophile *Moritella profunda* in complex with NADP<sup>+</sup> and folate. *Biomol. NMR Assign.* 7, 61–64.

(36) Loveridge, E. J., Tey, L. H., Behiry, E. M., Dawson, W. M., Evans, R. M., Whittaker, S. B. M., Günther, U. L., Williams, C., Crump, M. P., and Allemann, R. K. (2011) The Role of Large-Scale Motions in Catalysis by Dihydrofolate Reductase. *J. Am. Chem. Soc.* 133, 20561–20570.

(37) Osborne, M. J., Venkitakrishnan, R. P., Dyson, H. J., and Wright, P. E. (2003) Diagnostic chemical shift markers for loop conformation and substrate and cofactor binding in Dihydrofolate reductase complexes. *Protein Sci.* 12, 2230–2238.

(38) Williamson, M. P. (2013) Using chemical shift perturbation to characterise ligand binding. *Prog. Nucl. Magn. Reson. Spectrosc.* 73, 1–16.

(39) Ohmae, E., Sasaki, Y., and Gekko, K. (2001) Effects of Five-Tryptophan Mutations on Structure, Stability and function of *Escherichia coli* Dihydrofolate Reductase. *J. Biochem.* 2001, 130, 439–447.

(40) Ben-Bassat, A., Bauer, K., Chang, S. Y., Myambo, K., and Boosman, A. (1987) Processing of the initiation methionine from proteins: properties of the *Escherichia coli* methionine aminopeptidase and its gene structure. *J. Bacteriol.* 169, 751–757.

(41) Schnell, J. R., Dyson, H. J., and Wright, P. E. (2004) Structure, dynamics, and catalytic function of dihydrofolate reductase. *Annu. Rev. Biophys. Biomol. Struct.* 33, 119–140.

(42) Venkitakrishnan, R. P., Zaborowski, E., McElheny, D., Benkovic, S. J., Dyson, H. J., and Wright, P. E. (2004) Conformational changes in the active site loops of dihydrofolate reductase during the catalytic cycle. *Biochemistry* 43, 16046–16055.

(43) Hajduk, P. J., Augeri, D. J., Mack, J., Mendoza, R., Yang, J., Betz, S. F., and Fesik, S. W. (2000) NMR-based screening of proteins containing <sup>13</sup>C-labelled methyl groups. *J. Am. Chem. Soc.* 122, 7898–7904.

(44) Behiry, E. M., Evans, R. M., Guo, J., Loveridge, E. J., and Allemann, R. K. (2014) Loop Interactions During Catalysis by Dihydrofolate Reductase from *M. profunda*. *Biochemistry* 53, 4769–4774.

(45) Weikl, T. R., and Boehr, D. D. (2012) Conformational selection and induced changes along the catalytic cycle of *Escherichia coli* dihydrofolate reductase. *Proteins Struct. Funct. Bioinforma.* 80, 2369–2383.

(46) Boehr, D. D., Dyson, H. J., and Wright, P. E. (2008) Conformational Relaxation following Hydride Transfer Plays a Limiting Role in Dihydrofolate reductase Catalysis. *Biochemistry.* 47, 9227–9233.

(47) Mauldin, R. V., and Lee, A. L. (2010) NMR study of the role of M42 in the solution dynamics of *E. coli* dihydrofolate reductase. *Biochemistry.* 49, 1606–1615.

For Table of Contents Use Only

